Atmospheric
Chemistry
and Physics
Discussions

1   Formation of highly oxygenated organic molecules from chlorine atom

2   initiated oxidation of alpha-pinene

3

4   Yonghong Wang[1], Matthieu Riva[1,2], Hongbin Xie[3,1], Liine Heikkinen[1], Simon

5   Schallhart[1], Qiaozhi Zha[1], Chao Yan[1], Xucheng He[1], Otso Peräkylä[1] and Mikael Ehn[1]

6

7   [1]Institute for Atmospheric and Earth System Research / Physics, Faculty of Science, P.

8   O. Box 64, 00014 University of Helsinki, Helsinki, Finland

9   [2]Univ Lyon, Université Claude Bernard Lyon 1, CNRS, IRCELYON, F-69626,

10   Villeurbanne, France

11   [3]Key Laboratory of Industrial Ecology and Environmental Engineering (MOE), School

12   of Environmental Science and Technology, Dalian University of Technology, Dalian

13   116024, China

14

15   Submitted to: Atmospheric Chemistry and Physics

16

17   Corresponding to: Yonghong Wang and Hongbin Xie

18   yonghong.wang@helsinki.fi; hbxie@dlut.edu.cn

19

20

21

22

23

24

25

26

27

28

29   Abstract

30

31   Highly oxygenated organic molecules (HOMs) from atmospheric oxidation of alpha-

32   pinene can irreversibly condense to particles and contribute to secondary organic

33   aerosol (SOA) formation. Recently, the formation of nitryl chloride ($ClNO_2$) from

34   heterogeneous reactions, followed by its subsequent photolysis is suggested to be an

35   important source of chlorine atoms in many parts of the atmosphere. However, the

36   oxidation of monoterpenes such as alpha-pinene by chlorine atoms has received very

37   little attention, and the ability of this reaction to form HOM is completely unstudied.

38   Here, chamber experiments were conducted with alpha-pinene and chlorine under low

39   and high nitrogen oxide (NO_x) conditions. A NO_3-based CI-APi-TOF was used to

40   measure HOM products. Clear distributions of monomers with 9-10 carbon atoms and

41   dimers with 18-20 carbon atoms were observed under low NO_x conditions. With

42   increased concentration of NO_x within the chamber, the formation of dimers was

43   suppressed due to the reactions of peroxy radicals with NO. We estimated the HOM

44   yields from chlorine-initiated oxidation of alpha-pinene under low-NO_x conditions to

45   be around 1.8 %, though with a substantial uncertainty range (0.8-4 %) due to lack of

46   suitable calibration methods. Corresponding yields at high NO_x could not be

47   determined because of concurrent ozonolysis reactions. Our study demonstrates that

48   chlorine atoms also initiated oxidation of alpha-pinene and yields low volatility organic

49   compounds.

50

51

52

53

54

55

56

57

Atmospheric
Chemistry
and Physics
Discussions

1. Introduction

Highly oxygenated organic molecules (HOMs) have been identified as key species in the formation of new atmospheric aerosol particles and secondary organic aerosol (SOA) (Ehn et al., 2014, 2017; Kulmala et al., 2013; Bianchi et al., 2019). Recently, the formation of HOMs in the gas phase was described as an autoxidation process of peroxy radicals (RO_2) via multiple intramolecular H atom shifts (Crounse et al., 2013; Jokinen et al., 2014b; Mentel et al., 2015; Rissanen et al., 2014). Oxygen-containing moieties such as carbonyl, carboxylic acid and hydroxyl groups can weaken nearby C-H bonds, making H-abstraction and autoxidation competitive with bimolecular RO_2 reactions, e.g. with NO (Crounse et al., 2013; Praske et al., 2018). Until now, all studies on the formation of HOMs have focused on reactions initiated by oxygen-containing oxidants (O_3, OH and NO_3).

Increasing evidence indicates that the chlorine atom (Cl) may also play an important role in transforming atmospheric organics. (Tham et al., 2016; Thornton et al., 2010). Chlorine atoms have the greatest reactivity toward volatile organic compounds (VOC), with rate constants that are, with some exceptions, an order of magnitude higher than those of hydroxyl radicals (OH) (Riva et al., 2015). Historically, chlorine atoms were thought to be formed primarily from heterogeneous reaction cycles involving sea salt, and its concentration estimated to be around 1-10% of that of OH. Therefore, the role of chlorine atoms in atmospheric oxidation processes has traditionally been thought to be limited to the marine boundary layer only. In recent years, $ClNO_2$, as a significant chlorine atom source, was found in continental regions of America, Canada and Germany, and high concentrations of $ClNO_2$ were also detected in the urban atmosphere in China (Reyes-Villegas et al., 2018; Tham et al., 2016; Thornton et al., 2010; Wang et al., 2017). The new findings have expanded the potential importance of chlorine atoms from coastal areas to continental urban areas. A recent study also reported that chlorine atoms can be more important than OH radicals for the oxidation of alkanes in

87   the North China Plain (Liu et al., 2017). Therefore, it is desirable to probe the role of

88   chlorine radicals in the degradation of VOCs and related SOA formation.

89

90   Emission of biogenic volatile organic compounds (BVOC) to the atmosphere

91   dominates total hydrocarbon emissions on a global scale, with methane, isoprene and

92   terpenes having the highest source strengths (Guenther et al., 2012). Alpha-pinene is

93   the most abundant monoterpene in the atmosphere and its oxidation products from

94   ozonolysis and photooxidation contribute to a substantial fraction of SOA mass

95   (Riccobono et al., 2014; Zhang et al., 2018). Chlorine atom initiated reactions of alpha-

96   pinene have also been shown to contribute to the formation of SOA, which implies that

97   low volatile compounds are efficiently produced also in this process (Cai and Griffin,

98   2006; Ofner et al., 2013).

99

100 Similar to the reaction with OH radicals, the reaction of VOCs with chlorine atoms may

101 proceed either via addition of Cl to unsaturated bonds or via H-abstraction. Wang et.al

102 (2017) found that the Cl addition to isoprene can lead to the formation of low volatility

103 organic compounds. In principle, Cl-initiated reactions could form HOMs in a similar

104 manner as OH-initiated reactions (Berndt et al., 2016a), as the initial addition or

105 abstraction step is comparable for both oxidants. In view of the increased understanding

106 of the importance of chlorine atoms in atmospheric chemistry, it is desirable to

107 investigate the formation of HOMs from reactions of common atmospheric VOC with

108 Cl.

109

110 Here, a laboratory chamber experiments were performed to investigate the ability of

111 chlorine atom to form HOMs from the oxidation of alpha-pinene. HOMs were

112 characterized using a nitrate-based chemical ionization mass spectrometer, under both

113 low and high NO_x conditions. The yields of these HOMs were determined under the

114 low NO_x conditions, and the atmospheric implications of this study are discussed.

115

2. Experiment and method

2.1 experimental setup

The experiments were conducted in the "COALA" chamber at the University of Helsinki (Peräkylä et al., 2019; Riva et al., 2019). It is a 2 m³ Teflon chamber, run as a continuously stirred tank reactor, used with a flow of 45 liter per minutes (LPM), resulting in an average residence time of about 45 minutes. The chamber is surrounded by housing to provide dark conditions. No water vapor was added to the chamber, and the temperature was the same as the temperature of the room, around 25°C. A general schematic of the chamber facility is shown in Figure 1. Our experiment was aimed to probe chlorine atom initiated formation of HOMs under low/high NO_x conditions. We use 400 nm LED lights to photolyze chlorine and NO_2 and produce chlorine atoms and NO as following:

$$NO_2 \rightarrow NO + O$$
$$Cl_2 \rightarrow Cl + Cl$$
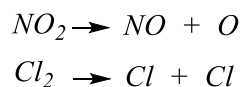
The concentration of Cl atoms was varied by changing the amount of 400 nm light. In practice this was done by turning on different amounts of the available lights, with the maximum corresponding to seven. We will refer below to the number of lights that were turned on, although each "light" corresponds to a group of LED strips.

2.2 Instrumentation and data analysis

A nitrate ion (NO_3^-) based chemical ionization atmospheric pressure interface long time-of-flight (CI-APi-L-TOF) mass spectrometer was used for measuring HOMs. The instrument has been shown to be sensitive towards such group of compounds, detecting them as adducts with the nitrate ion. Due to a lack of suitable calibration methods, the CI-APi-L-TOF was not calibrated for HOMs during this study. In order to estimate rough HOM concentrations, we directly use the calibration coefficient (C = 1.6 e10) utilized by Ehn et al. (2014), which is very close to values utilized in several other

143 studies using a CI-APi-TOF(Jokinen et al., 2014a; Riva et al., 2019). This approach

144 obviously brings large uncertainties when the estimating HOM concentrations, which

145 we estimate to be at least -50 %/+100 %. More detailed information about the

146 instrument can be found in (Jokinen et al., 2012), noting that compared with the CI-

147 APi-TOF used before, the long time-of-flight mass spectrometer used here has a

148 doubled mass resolving power enabling a more accurate assignment of molecular

149 formulas. Simultaneously, we also used a high-resolution long time-of-flight aerosol

150 mass spectrometer (HR-L-TOF-AMS) to measure bulk aerosol chemical properties

151 (Decarlo et al., 2006). As no seed aerosol particles were added to the chamber, the VOC

152 oxidation products lead to new particle formation and growth to large enough sizes to

153 be measured by the AMS. We also periodically used a filter in front of the AMS inlet to

154 see the influence of the background signal to measured aerosol mass concentration.

155 There were 10 minutes of filter measurements per hour during our experiments. A PTR-

156 TOF-MS (TOF-8000, Ionicon) was used to measure the concentration of alpha-pinene

157 in the chamber. The instrument background was determined every day for 20 mins by

158 guiding the chamber air through a catalytic converter, which removes the VOCs. Then,

159 the background corrected signals were used to obtain alpha-pinene mixing ratios by

160 using the calibration coefficient determined before the experiments. A description of

161 the used setup employed for the calibration and zero air measurements have been

162 introduced earlier (Schallhart et al., 2018). A custom-built DMPS system was used to

163 measure the particle number size distribution from 10 nm to 400 nm in the chamber.

164 The NO concentration was measured with an ECO-PHYSICS CLD 780 TR instrument

165 with a detection limit of 3 ppt. NO_x (=NO+NO_2) concentrations were determined by

166 using a Thermo-Fisher 42i analyzer. O_3 concentration was measured with a Thermo-

167 Fisher 49i analyzer.

168

2.2 Estimation of chlorine atom concentrations

170 During steady state in the chamber, average concentrations of chlorine atom was

171 calculated using the rate coefficients (4.6±1.3) • 10^{-10} cm^3 molecule $^{-1}$ s^{-1} of Cl atoms

172 with alpha-pinene (Finlayson-Pitts et al., 1999), as following:

173 $$d[AP]/dt = Q\_in - k * [Cl] * [AP] - Q\_out$$

174 where Q_in is the concentration of alpha-pinene continuously injected into the chamber,

175 and Q_out is the concentration that exited the chamber. The term Q_in was 13.3 ppb,

176 while the term Q_out varied depending on the conditions, and is calculated as $[AP]/45$

177 min. During steady state, $d[AP]/dt$ is zero, and then $[Cl]$ concentration is calculated

178 accordingly. As shown in Figure 2, the concentration of HOMs decreased and alpha-

179 pinene increased as the number of lights switched on changed from 7 to 4, 2 and 1. We

180 use the variation of alpha-pinene and HOM concentrations during this run to calculate

181 both chlorine atom concentrations and HOM yields. Each change in alpha-pinene

182 concentration was due to the change in Cl atom concentration, and with knowledge of

183 the reaction rate, the concentration of Cl atoms as a function of the number of lights

184 turned on was determined (Figure 3). The calculated $[Cl]$ concentrations are in the range

185 of $(1-5) \times 10^5$ molecules cm^{-3}, which is within atmospheric relevant concentration

186 ranges (Tham et al., 2016). Raw data from the CI-API-L-TOF were recorded in 10s

187 resolution in HDF format. We used Toftools for data analysis and detailed protocols of

188 the software have been introduced by Junninen et al. (2010).

189

190 ## 2.3 HOMs molar yield

191

192 The change of HOM concentration with time can be described as follows, in analogy

193 with Ehn et al. (2014):

194

195 $$\frac{d[HOMs]}{dt} = k_1 g[a - pinene][Cl] - k_{loss}[HOMs] \qquad (1)$$

196

197

198 $$g = \frac{k_{loss}[HOMs]}{k_1[a - pinene][Cl]} \qquad (2)$$

Atmospheric
Chemistry
and Physics
Discussions

Open Access

EGU

199

200   Here, k_1 is the reaction rate coefficient of alpha-pinene with chlorine atoms and γ is the

201   molar yield of HOMs, i.e., the fraction of alpha-pinene + Cl reactions that produced

202   HOMs. k_{loss} is the loss rate of HOMs to the chamber walls and particles, though the

203   latter was negligible in this study due to the low aerosol loadings. We used 300 s as a

204   lifetime of HOMs, i.e. $k_{loss} = 1/300$ s^{-1}, in our previous study in the COALA chamber

205   (Riva et al., 2019).

206

207   3. Results and discussion

208   3.1 Formation of HOMs under low NO condition

209

210   Figure 4 (a, b, c and d) shows mass spectra measured by the NO$_3$-CI-APi-TOF during

211   steady state alpha-pinene oxidation with different amounts of lights switched on. The

212   x-axis represents mass to charge ratio, in units of Thomson (Th). The y-axis represents

213   signals in units of counts per second. As we can see, both monomers (280-400 Th) and

214   dimers (440-580 Th) showed increased signals with increased number of lights, and

215   consequently increased [Cl]. The most abundant peaks are labeled in Figure 4d, with

216   some of the largest signals in the monomer range attributed to $C_9H_{12}O_{7,8}$ and

217    $C_{10}H_{14}O_{8,9,10}$. During the oxidation of $C_{10}H_{16}$, in the absence of NO, the fate of RO$_2$

218   radicals depends on the concentrations of HO$_2$ and RO$_2$. Autoxidation competes with

219   bimolecular reactions, becoming more likely at lower RO$_2$ and HO$_2$ concentrations. At

220   high oxidation rates, autoxidation is likely inhibited compared to actual atmospheric

221   conditions.

222

223   As we show in the Figure 4(d), $C_{10}H_{14}O_{8-12}$ compounds are large peaks in the monomer

224   range observed with the NO$_3$-CI-API-TOF. These compounds with 14 hydrogens may

225   come from decomposition of $C_{10}H_{15}O_n$ peroxy radicals via loss of OH or HO$_2$, or

226   following reactions with other RO$_2$, as depicted schematically in Figure 5. Another

227   abundant group is $C_{10}H_{16}O_{6-12}$, which may result from RO_2 terminated by HO_2. In the

228   dimer range, the most abundant compounds are $C_{19}H_{28}O_{8-14}$ and $C_{20}H_{30}O_{11-14}$. These

229   compounds come from RO_2 cross reactions, as has been shown in multiple earlier

230   studies. The $C_{20}H_{30}O_n$ dimers are most likely formed from reactions of two $C_{10}H_{15}O_x$

231   radicals, as were many abundant monomers. As noted earlier, Cl oxidation of alkenes

232   may occur via a Cl addition (forming an initial radical containing 16 H-atoms and one

233   Cl atom) or via an H-abstraction reaction (forming a radical with 15 H-atoms and no

234   Cl) (Figure 5). Based on our HOM spectra, the abstraction reaction would seem to

235   completely dominate the reaction, as only a few minor peaks in the spectrum could be

236   identified to contain Cl. Alternatively, only the abstraction pathway leads to HOM

237   formation, or the Cl atom is lost during the subsequent reaction in the oxidation

238   processes. With our data, we cannot rule out either of these explanations for this

239   surprising result. Loss of HCl from alpha-pinene products from Cl oxidation have, to

240   our knowledge, only been reported to take place in the aerosol phase (Ofner2013).

241

242   Figure 6 shows the variation of several closed-shell HOM products and the peroxy

243   radical $C_{10}H_{15}O_{10}$ measured by NO_3-CI-API-TOF when we changed the lights from

244   dark conditions to 1, 2, 4 and 7 lights switched on. Given the low Cl atom concentration,

245   it is expected that no multi-generation oxidation by Cl can take place, and the behavior

246   of all closed shell oxidation products should follow similar patterns. As seen in Figure

247   6, this was the case both for monomers and dimers. The less steep increase of the radical

248   is also according to expectations, as the formation of RO_2 is linear with the alpha-pinene

249   oxidation rate, but the loss rate (when dominated by RO_2 cross reactions) is proportional

250   to $(RO_2)^2$. For closed shell species, the wall loss-driven loss rate stays constant

251   throughout the experiment, and therefore they increase linearly with the alpha-pinene

252   oxidation rate while the RO_2 radicals increase as the square root of the oxidation rate.

253   For more detailed discussion on RO_2 dynamics in a steady state chamber, see Ehn et al.

254   (2014).

255

Atmospheric
Chemistry
and Physics
Discussions

Open Access

EGU

256   In Figure7, we plotted time series of the particle number size distribution and the total

257   number concentration, together with mass concentrations of particulate chloride and

258   organics as we changed the number of lights. Particle formation was detected even at

259   the lowest Cl atom concentration, as indicated by the increases in aerosol number

260   concentration. An increased in aerosol mass concentration as detected by the AMS only

261   took place at the two highest Cl atom concentrations, when the particles were able to

262   grow into a size range measurable by the AMS. Particulate chloride mass

263   concentrations also increased relatively linearly with the concentration of organics as

264   we increased the number of lights. The Chl/Org ratio was only around 3 %, suggesting

265   that the majority of condensed OVOC did not contain Cl atoms. Some part of the

266   chloride signal may also result from adsorption of HCl to particles.

267

268   ## 3.2 Formation of HOMs at high NOx

269

270   Anthropogenic emissions have a significant influence on the formation of SOA, to a

271   large part due to the influence of NO_x on the atmospheric oxidation chemistry (Lee et

272   al., 2016). In general, the fate of peroxy radicals in chamber experiments can be

273   dominated by reactions with other RO_2, HO_2 or NO, depending on the exact conditions.

274   In our experiments without NO_x addition, RO_2 was expected to be the main terminator,

275   as also supported by the high number of detected ROOR dimers. In the atmosphere, all

276   of the three mentioned reaction partners may be relevant at the same time. However,

277   with increased anthropogenic influence, the reaction of RO_2 with NO will often become

278   dominant. Therefore, we added NO_x to the chamber as it allowed for the isolation of

279   the formation pathways leading to HOMs in cases where NO was the main terminator

280   for RO_2 radicals. Figure 8 depicts a HOM mass spectrum at steady state during alpha-

281   pinene oxidation by chlorine radicals in the presence of ~10 ppb NO_x, with the

282   maximum 7 lights turned on. As anticipated, the dimers above 440 Th were greatly

283   reduced compared to the runs without NO_x. As more lights were turned on, both the Cl

284   atoms and NO formation increased, as the 400 nm lights photolyze both Cl_2 and NO_2.

Atmospheric
Chemistry
and Physics
Discussions
Open Access
EGU

285   This coupling, together with the fact that the NO_2 photolysis leads to ozone formation,

286   which subsequently can react with alpha-pinene to form HOMs, limits our quantitative

287   analysis of these experiments. However, we conclude that efficient HOM formation

288   took place also under these high-NOx conditions, and thus the autoxidation occurs

289   rapidly enough to still compete with RO_2 termination reactions. The NO_x addition also

290   formed an abundance of organonitrate compounds like $C_{10}H_{15}NO_{8,9,10,11,12}$, as shown in

291   Figure 8. This family of compounds may form from H-abstraction by the chlorine

292   radical, followed by autoxidation and finally radical termination by NO. The concurrent

293   formation of ozone means that also some alpha-pinene ozonolysis reaction will take

294   place, though oxidation by Cl atoms was still the main loss for alpha-pinene also under

295   these conditions.

296

297   Figure 9 shows variation of some nitrogen-containing HOMs and variation of alpha-

298   pinene, ozone, NO and NO_x, as we changed the lights from dark conditions to 1, 2, 4

299   or 7 lights switched on. The concentrations of alpha-pinene and NO_2 decreased because

300   of the consumption by chlorine radicals and photolysis of NO_2 into NO. Importantly,

301   we did not observe any SOA when we had NO in the chamber. NO may have suppressed

302   the particle formation by suppressing the dimer formation, as these have been shown to

303   be important for initial particle formation (Tröstl et al., 2016).

304

305   ## 3.2 Estimated HOMs production yields

306

307   Quantifying the molar yields of HOMs is essential to know their potential importance

308   from a specific system. We attempt to estimate the molar yield in the case of Cl

309   oxidation of alpha-pinene in the absence of NO_x. The initial $C_{10}H_{16}$ concentration is

310   around 13.3 ppb without any UV lights switched on in the chamber. As we changed the

311   lights, alpha-pinene and HOM concentrations varied as we showed in Figure 3. In

312   addition, we calculated the concentration of Cl radicals as introduced in the Methods

313   section. With this information, we can calculate the formation rate of HOM, which in

314   steady state equals the HOM loss rate [HOM]*k_{loss}. We can also calculate the oxidation

315   rate of alpha-pinene as [alpha-pinene]*[Cl]*k_{AP+Cl}. The ratio of these two numbers

316   corresponds to the HOM molar yield. We selected the same runs as in Fig. 3, used also

317   for calculating the chlorine radical concentration, and calculated the ratio as a linear fit

318   to these four conditions (Figure 10). We get a slope of 0.018, meaning a HOM yield of

319   1.8%. Considering the uncertainty in estimating absolute HOM concentrations, we

320   conservatively estimate that the molar HOM yield from alpha-pinene + Cl is within the

321   range of 0.8-4 %. These values are similar to HOM yields reported for alpha-pinene

322   oxidation by ozone and OH (Berndt et al., 2016; Ehn et al., 2014).

323

324   4.Conclusion

325

326   We have systematically explored the reactions of alpha-pinene with chlorine atoms in

327   a simulation smog chamber under atmospherically relevant conditions. We measured

328   substantial amounts of highly oxidized organic molecules (HOM) with a NO_3-CI-API-

329   TOF. With increasing UV lights, and consequently higher chlorine radical

330   concentrations, the concentrations of both HOM and secondary organic aerosol

331   increased. With addition of NOx, HOM monomer formation was still efficient, but the

332   particle formation decreased greatly. We estimated HOM molar yields of around 1.8 %

333   (0.8-4 %) from the reaction of alpha-pinene with Cl atoms. Our study thus indicates

334   that in regions where chlorine atom oxidation is of importance, its possible reactions

335   with monoterpenes can be an important source of HOM, and consequently, SOA.

336

Atmospheric
Chemistry
and Physics
Discussions

341 providing the software.

342

343 **Competing financial interests**

344 The authors declare no competing financial interests.

345

346 **Author contributions**

347 Y. H. W, H. B. X and M. E had the original idea of the study. Y. H. W, M. R and H. B.

348 X conducted the chamber experiments. Y. H. W, M. R, H. B. X, L.H and M. E

349 interpreted the data. Y.H.W plotted the figures, wrote the manuscript with comments

350 and suggestions from all co-authors.

351

352

353

354

355

356

357

358

359

360

361

362

363

Reference

365 Berndt, T., Richters, S., Jokinen, T., Hyttinen, N., Kurtén, T., Otkjaer, R. V,

366 Kjaergaard, H. G., Stratmann, F., Herrmann, H., Sipilä, M., Kulmala, M. and Ehn, M.:

367 ARTICLE Hydroxyl radical-induced formation of highly oxidized organic

368 compounds, , doi:10.1038/ncomms13677, 2016a.

369 Berndt, T., Richters, S., Jokinen, T., Hyttinen, N., Kurtén, T., Otkjær, R. V,

370 Kjaergaard, H. G., Stratmann, F., Herrmann, H., Sipilä, M., Kulmala, M. and Ehn, M.:

371 Hydroxyl radical-induced formation of highly oxidized organic compounds, Nature

372 Communications, 7, 13677 [online] Available from:

373 https://doi.org/10.1038/ncomms13677, 2016b.

374 Bianchi, F., Kurtén, T., Riva, M., Mohr, C., Rissanen, M. P., Roldin, P., Berndt, T.,

375 Crounse, J. D., Wennberg, P. O., Mentel, T. F., Wildt, J., Junninen, H., Jokinen, T.,

376 Kulmala, M., Worsnop, D. R., Thornton, J. A., Donahue, N., Kjaergaard, H. G. and

377 Ehn, M.: Highly Oxygenated Organic Molecules (HOM) from Gas-Phase

378 Autoxidation Involving Peroxy Radicals: A Key Contributor to Atmospheric Aerosol,

379 Chemical Reviews, 119(6), 3472–3509, doi:10.1021/acs.chemrev.8b00395, 2019.

380 Cai, X. and Griffin, R. J.: Secondary aerosol formation from the oxidation of biogenic

381 hydrocarbons by chlorine atoms, Journal of Geophysical Research Atmospheres,

382 111(14), 1–14, doi:10.1029/2005JD006857, 2006.

383 Crounse, J. D., Nielsen, L. B., Jørgensen, S., Kjaergaard, H. G. and Wennberg, P. O.:

384 Autoxidation of organic compounds in the atmosphere, Journal of Physical Chemistry

385 Letters, 4(20), 3513–3520, doi:10.1021/jz4019207, 2013.

386 Decarlo, P. F., Kimmel, J. R., Trimborn, A., Northway, M. J., Jayne, J. T., Aiken, A.

387 C., Gonin, M., Fuhrer, K., Horvath, T., Docherty, K. S., Worsnop, D. R. and Jimenez,

388 J. L.: Field-Deployable, High-Resolution, Time-of-Flight Aerosol Mass Spectrometer,

389 Analytical Chemistry, 78, 8281–8289, doi:10.1021/ac061249n, 2006.

390   Ehn, M., Thornton, J. A., Kleist, E., Sipilä, M., Junninen, H., Pullinen, I., Springer,

391   M., Rubach, F., Tillmann, R., Lee, B., Lopez-Hilfiker, F., Andres, S., Acir, I.-H.,

392   Rissanen, M., Jokinen, T., Schobesberger, S., Kangasluoma, J., Kontkanen, J.,

393   Nieminen, T., Kurtén, T., Nielsen, L. B., Jørgensen, S., Kjaergaard, H. G.,

394   Canagaratna, M., Maso, M. D., Berndt, T., Petäjä, T., Wahner, A., Kerminen, V.-M.,

395   Kulmala, M., Worsnop, D. R., Wildt, J. and Mentel, T. F.: A large source of low-

396   volatility secondary organic aerosol, Nature, 506(7489), 476–479,

397   doi:10.1038/nature13032, 2014a.

398   Ehn, M., Thornton, J. A., Kleist, E., Sipilä, M., Junninen, H., Pullinen, I., Springer,

399   M., Rubach, F., Tillmann, R., Lee, B., Lopez-Hilfiker, F., Andres, S., Acir, I.-H.,

400   Rissanen, M., Jokinen, T., Schobesberger, S., Kangasluoma, J., Kontkanen, J.,

401   Nieminen, T., Kurtén, T., Nielsen, L. B., Jørgensen, S., Kjaergaard, H. G.,

402   Canagaratna, M., Dal Maso, M., Berndt, T., Petäjä, T., Wahner, A., Kerminen, V.-M.,

403   Kulmala, M., Worsnop, D. R., Wildt, J. and Mentel, T. F.: A large source of low-

404   volatility secondary organic aerosol, Nature, 506, doi:10.1038/nature13032, 2014b.

405   Ehn, M., Berndt, T., Wildt, U. and Mentel, T.: Highly Oxygenated Molecules from

406   Atmospheric Autoxidation of Hydrocarbons: A Prominent Challenge for Chemical

407   Kinetics Studies, International journal of chemical knineticsinetics, 821–831,

408   doi:10.1002/kin.21130, 2017.

409   Finlayson-Pitts, B. J., Keoshian, C. J., Buehler, B. and Ezell, A. A.: Kinetics of

410   Reaction of Chlorine Atoms with Some, International Journal of Chemical Kinetics,

411   31, 491–499, 1999.

412   Guenther, A., Hewitt, C. N., Erickson, D., Fall, R., Geron, C., Graedel, T., Harley, P.,

413   Klinger, L., Lerdau, M., Mckay, W. A., Pierce, T., Scholes, B., Steinbrecher, R.,

414   Tallamraju, R., Taylor, J. and Zimmerman, P.: A global model of natural volatile

415   organic compound emissions, Journal of Geophysical Research: Atmospheres,

416   100(D5), 8873–8892, doi:10.1029/94JD02950, 1995.

417   Jokinen, T., Sipilä, M., Junninen, H., Ehn, M., Lönn, G., Hakala, J., Petäjä, T.,

418   Mauldin Iii, R. L., Kulmala, M. and Worsnop, D. R.: Atmospheric sulphuric acid and

419   neutral cluster measurements using CI-APi-TOF, Atmos. Chem. Phys. Atmospheric

420   Chemistry and Physics, 12, 4117–4125, doi:10.5194/acp-12-4117-2012, 2012.

421   Jokinen, T., Sipilä, M., Richters, S., Kerminen, V., Paasonen, P., Stratmann, F.,

422   Worsnop, D., Kulmala, M., Ehn, M., Herrmann, H. and Berndt, T.: Rapid

423   Autoxidation Forms Highly Oxidized RO 2 Radicals in the Atmosphere **

424   Angewandte, , 1–6, doi:10.1002/anie.201408566, 2014a.

425   Jokinen, T., Sipilä, M., Richters, S., Kerminen, V. M., Paasonen, P., Stratmann, F.,

426   Worsnop, D., Kulmala, M., Ehn, M., Herrmann, H. and Berndt, T.: Rapid

427   autoxidation forms highly oxidized RO2 radicals in the atmosphere, Angewandte

428   Chemie - International Edition, 53(52), 14596–14600, doi:10.1002/anie.201408566,

429   2014b.

430   Kulmala, M., Kontkanen, J., Junninen, H., Lehtipalo, K., Manninen, H. E., Nieminen,

431   T., Petaja, T., Sipila, M., Schobesberger, S., Rantala, P., Franchin, A., Jokinen, T.,

432   Jarvinen, E., Aijala, M., Kangasluoma, J., Hakala, J., Aalto, P. P., Paasonen, P.,

433   Mikkila, J., Vanhanen, J., Aalto, J., Hakola, H., Makkonen, U., Ruuskanen, T.,

434   Mauldin, R. L., Duplissy, J., Vehkamaki, H., Back, J., Kortelainen, A., Riipinen, I.,

435   Kurten, T., Johnston, M. V., Smith, J. N., Ehn, M., Mentel, T. F., Lehtinen, K. E. J.,

436   Laaksonen, A., Kerminen, V.-M. and Worsnop, D. R.: Direct Observations of

437   Atmospheric Aerosol Nucleation, Science, 339(6122), 943–946,

438   doi:10.1126/science.1227385, 2013.

439   Lee, B. H., Mohr, C., Lopez-Hilfiker, F. D., Lutz, A., Hallquist, M., Lee, L., Romer,

440   P., Cohen, R. C., Iyer, S., Kurtén, T., Hu, W., Day, D. A., Campuzano-Jost, P.,

441   Jimenez, J. L., Xu, L., Ng, N. L., Guo, H., Weber, R. J., Wild, R. J., Brown, S. S.,

442   Koss, A., de Gouw, J., Olson, K., Goldstein, A. H., Seco, R., Kim, S., McAvey, K.,

443   Shepson, P. B., Starn, T., Baumann, K., Edgerton, E. S., Liu, J., Shilling, J. E., Miller,

444   D. O., Brune, W., Schobesberger, S., D'Ambro, E. L. and Thornton, J. A.: Highly

445   functionalized organic nitrates in the southeast United States: Contribution to

446   secondary organic aerosol and reactive nitrogen budgets, Proceedings of the National

447   Academy of Sciences, 113(6), 1516–1521, doi:10.1073/pnas.1508108113, 2016.

448 Liu, X., Qu, H., Huey, L. G., Wang, Y., Sjostedt, S., Zeng, L., Lu, K., Wu, Y., Hu,

449 M., Shao, M., Zhu, T. and Zhang, Y.: High Levels of Daytime Molecular Chlorine

450 and Nitryl Chloride at a Rural Site on the North China Plain, Environ Sci Technol, 51,

451 9588–9595, doi:10.1021/acs.est.7b03039, 2017.

452 Mentel, T. F., Springer, M., Ehn, M., Kleist, E., Pullinen, I., Kurtén, T., Rissanen, M.,

453 Wahner, A. and Wildt, J.: Formation of highly oxidized multifunctional compounds:

454 autoxidation of peroxy radicals formed in the ozonolysis of alkenes – deduced from

455 structure–product relationships, Atmos. Chem. Phys, 15, 6745–6765,

456 doi:10.5194/acp-15-6745-2015, 2015.

457 Ofner, J., Kamilli, K. A., Held, A., Lendl, B. and Zetzsch, C.: Halogen-induced

458 organic aerosol (XOA): a study on ultra-fine particle formation and time-resolved

459 chemical characterization, Faraday Discussions, 165, 135, doi:10.1039/c3fd00093a,

460 2013.

461 Peräkylä, O., Riva, M., Heikkinen, L., Quéléver, L., Roldin, P. and Ehn, M.:

462 Experimental investigation into the volatilities of highly oxygenated organic

463 molecules (HOM), , (July), 1–28, 2019.

464 Praske, E., Otkjær, R. V, Crounse, J. D., Hethcox, J. C., Stoltz, B. M., Kjaergaard, H.

465 G. and Wennberg, P. O.: Atmospheric autoxidation is increasingly important in urban

466 and suburban North America, Proceedings of the National Academy of Sciences,

467 115(1), 64 LP – 69, doi:10.1073/pnas.1715540115, 2018.

468 Reyes-Villegas, E., Priestley, M., Ting, Y.-C., Haslett, S., Bannan, T., Le Breton, M.,

469 Williams, P. I., Bacak, A., Flynn, M. J., Coe, H., Percival, C. and Allan, J. D.:

470 Simultaneous aerosol mass spectrometry and chemical ionisation mass spectrometry

471 measurements during a biomass burning event in the UK: insights into nitrate

472 chemistry, Atmos. Chem. Phys, 185194, 4093–4111, doi:10.5194/acp-18-4093-2018,

473 2018.

474 Riccobono, F., Schobesberger, S., Scott, C. E., Dommen, J., Ortega, I. K., Rondo, L.,

475 Almeida, J., Amorim, A., Bianchi, F., Breitenlechner, M., David, A., Downard, A.,

476 Dunne, E. M., Duplissy, J., Ehrhart, S., Flagan, R. C., Franchin, A., Hansel, A.,

Junninen, H., Kajos, M., Keskinen, H., Kupc, A., Kürten, A., Kvashin, A. N.,
Laaksonen, A., Lehtipalo, K., Makhmutov, V., Mathot, S., Nieminen, T., Onnela, A.,
Petäjä, T., Praplan, A. P., Santos, F. D., Schallhart, S., Seinfeld, J. H., Sipilä, M.,
Spracklen, D. V, Stozhkov, Y., Stratmann, F., Tomé, A., Tsagkogeorgas, G.,
Vaattovaara, P., Viisanen, Y., Vrtala, A., Wagner, P. E., Weingartner, E., Wex, H.,
Wimmer, D., Carslaw, K. S., Curtius, J., Donahue, N. M., Kirkby, J., Kulmala, M.,
Worsnop, D. R. and Baltensperger, U.: Oxidation Products of Biogenic Emissions
Contribute to Nucleation of Atmospheric Particles, Science, 344(717),
doi:10.1126/science.1243527, 2014.

Rissanen, M. P., Kurtén, T., Sipilä, M., Thornton, J. A., Kangasluoma, J., Sarnela, N.,
Junninen, H., Jørgensen, S., Schallhart, S., Kajos, M. K., Taipale, R., Springer, M.,
Mentel, T. F., Ruuskanen, T., Petäjä, T., Worsnop, D. R., Kjaergaard, H. G. and Ehn,
M.: The formation of highly oxidized multifunctional products in the ozonolysis of
cyclohexene, Journal of the American Chemical Society, 136(44), 15596–15606,
doi:10.1021/ja507146s, 2014.

Riva, M., Healy, R. M., Flaud, P. M., Perraudin, E., Wenger, J. C. and Villenave, E.:
Gas- and Particle-Phase Products from the Chlorine-Initiated Oxidation of Polycyclic
Aromatic Hydrocarbons, Journal of Physical Chemistry A, 119(45), 11170–11181,
doi:10.1021/acs.jpca.5b04610, 2015.

Riva, M., Heikkinen, L., Bell, D. M., Peräkylä, O., Zelenyuk, A. and Ehn, M.:
Chemical transformations in monoterpene-derived organic aerosol enhanced by
inorganic composition, npj Climate and Atmospheric Science, (July 2018), 1–9,
doi:10.1038/s41612-018-0058-0, 2019a.

Riva, M., Rantala, P., Krechmer, E. J., Peräkylä, O., Zhang, Y., Heikkinen, L.,
Garmash, O., Yan, C., Kulmala, M., Worsnop, D. and Ehn, M.: Evaluating the
performance of five different chemical ionization techniques for detecting gaseous
oxygenated organic species, Atmospheric Measurement Techniques, 12(4), 2403–
2421, doi:10.5194/amt-12-2403-2019, 2019b.

Schallhart, S., Rantala, P., Kajos, M. K., Aalto, J., Mammarella, I., Ruuskanen, T. M.

506   and Kulmala, M.: Temporal variation of VOC fluxes measured with PTR-TOF above

507   a boreal forest, Atmospheric Chemistry and Physics, 18(2), 815–832,

508   doi:10.5194/acp-18-815-2018, 2018.

509   Tham, Y. J., Wang, Z., Li, Q., Yun, H., Wang, W., Wang, X., Xue, L., Lu, K., Ma, N.,

510   Bohn, B., Li, X., Kecorius, S., Größ, J., Shao, M., Wiedensohler, A., Zhang, Y. and

511   Wang, T.: Significant concentrations of nitryl chloride sustained in the morning:

512   investigations of the causes and impacts on ozone production in a polluted region of

513   northern China, Atmos. Chem. Phys, 16, 14959–14977, doi:10.5194/acp-16-14959-

514   2016, 2016.

515   Thornton, J. A., Kercher, J. P., Riedel, T. P., Wagner, N. L., Cozic, J., Holloway, J.

516   S., Dubé, W. P., Wolfe, G. M., Quinn, P. K., Middlebrook, A. M., Alexander, B. and

517   Brown, S. S.: A large atomic chlorine source inferred from mid-continental reactive

518   nitrogen chemistry, Nature, 464(7286), 271–274, doi:10.1038/nature08905, 2010a.

519   Thornton, J. A., Kercher, J. P., Riedel, T. P., Wagner, N. L., Cozic, J., Holloway, J.

520   S., Dubé, W. P., Wolfe, G. M., Quinn, P. K., Middlebrook, A. M., Alexander, B. and

521   Brown, S. S.: A large atomic chlorine source inferred from mid-continental reactive

522   nitrogen chemistry, Nature, 464(7286), 271–274, doi:10.1038/nature08905, 2010b.

523   Tröstl, J., Chuang, W. K., Gordon, H., Heinritzi, M., Yan, C., Molteni, U., Ahlm, L.,

524   Frege, C., Bianchi, F., Wagner, R., Simon, M., Lehtipalo, K., Williamson, C., Craven,

525   J. S., Duplissy, J., Adamov, A., Almeida, J., Bernhammer, A.-K., Breitenlechner, M.,

526   Brilke, S., Dias, A., Ehrhart, S., Flagan, R. C., Franchin, A., Fuchs, C., Guida, R.,

527   Gysel, M., Hansel, A., Hoyle, C. R., Jokinen, T., Junninen, H., Kangasluoma, J.,

528   Keskinen, H., Kim, J., Krapf, M., Kürten, A., Laaksonen, A., Lawler, M., Leiminger,

529   M., Mathot, S., Möhler, O., Nieminen, T., Onnela, A., Petäjä, T., Piel, F. M.,

530   Miettinen, P., Rissanen, M. P., Rondo, L., Sarnela, N., Schobesberger, S., Sengupta,

531   K., Sipilä, M., Smith, J. N., Steiner, G., Tomè, A., Virtanen, A., Wagner, A. C.,

532   Weingartner, E., Wimmer, D., Winkler, P. M., Ye, P., Carslaw, K. S., Curtius, J.,

533   Dommen, J., Kirkby, J., Kulmala, M., Riipinen, I., Worsnop, D. R., Donahue, N. M.

534   and Baltensperger, U.: The role of low-volatility organic compounds in initial particle

535   growth in the atmosphere, Nature, 533(7604), 527–531, doi:10.1038/nature18271,

536   2016.

537   Wang, Z., Wang, W., Tham, Y. J., Li, Q., Wang, H., Wen, L., Wang, X. and Wang,

538   T.: Fast heterogeneous N_2O_5 uptake and $ClNO_2$ production in power plant and

539   industrial plumes observed in the nocturnal residual layer over the North China Plain,

540   Atmos. Chem. Phys, 175194, 12361–12378, doi:10.5194/acp-17-12361-2017, 2017.

541   Zhang, H., Yee, L. D., Lee, B. H., Curtis, M. P., Worton, D. R., Isaacman-VanWertz,

542   G., Offenberg, J. H., Lewandowski, M., Kleindienst, T. E., Beaver, M. R., Holder, A.

543   L., Lonneman, W. A., Docherty, K. S., Jaoui, M., Pye, H. O. T., Hu, W., Day, D. A.,

544   Campuzano-Jost, P., Jimenez, J. L., Guo, H., Weber, R. J., de Gouw, J., Koss, A. R.,

545   Edgerton, E. S., Brune, W., Mohr, C., Lopez-Hilfiker, F. D., Lutz, A., Kreisberg, N.

546   M., Spielman, S. R., Hering, S. V., Wilson, K. R., Thornton, J. A. and Goldstein, A.

547   H.: Monoterpenes are the largest source of summertime organic aerosol in the

548   southeastern United States, Proceedings of the National Academy of Sciences,

549   201717513, doi:10.1073/pnas.1717513115, 2018.

550

551

552

553

554

555

556

557

558

559

560

561

562

563   Figure and table captions

564

565
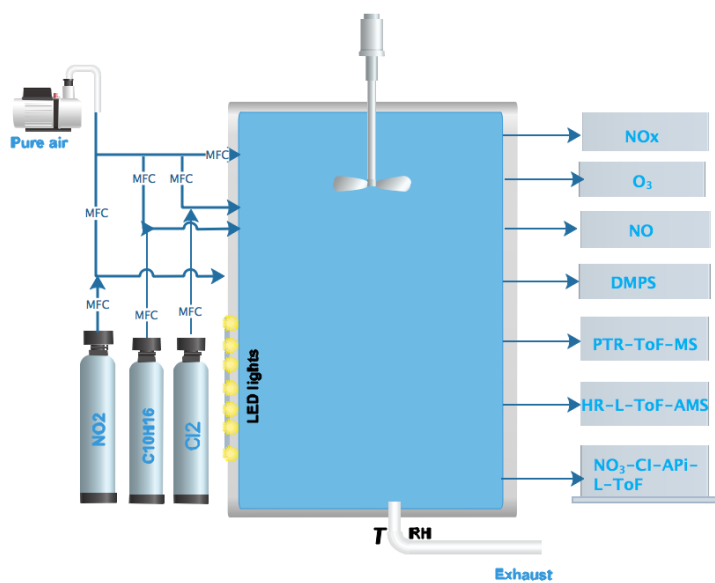
566
567   Figure 1 A schematic of the chamber setup and instruments used in the experiment.

568

569

570

571

572

573

574

575

576

577

578

579

580   Figure 2. The variation of total HOM concentration and alpha-pinene during four

581   experiments where the 400 nm lights were decreased stepwise from 7 lights to 4, 2
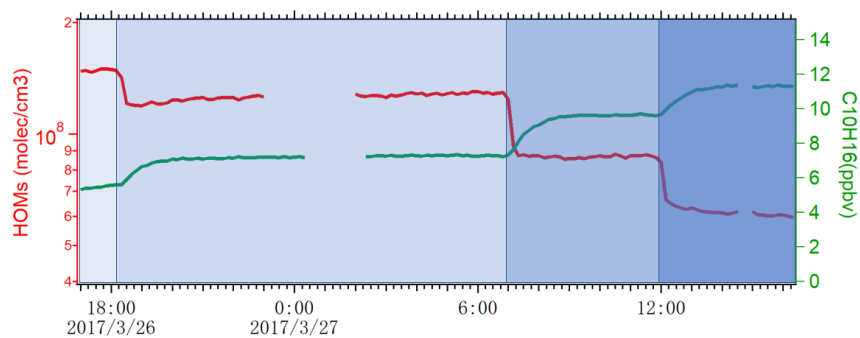
582   and 1 light, respectively.

583

584

585

586

587

588

589

590

591
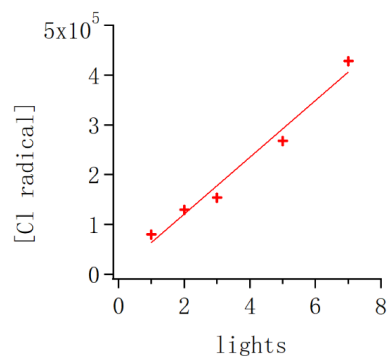
Figure 3. The variation of chlorine radical concentration as a function of lights. The

input alpha-pinene concentration was kept constant throughout the experiments.

594

595

596

597

598

599

600

601

602

603

604

605

606

607

608

609

Atmospheric
Chemistry
and Physics
Discussions

Open Access

EGU
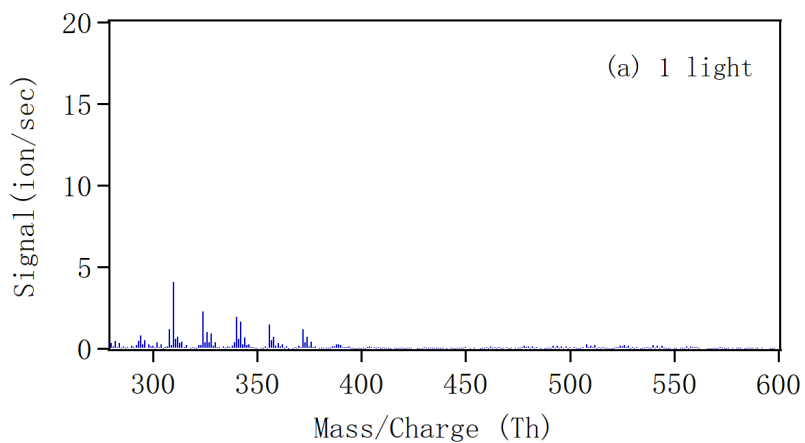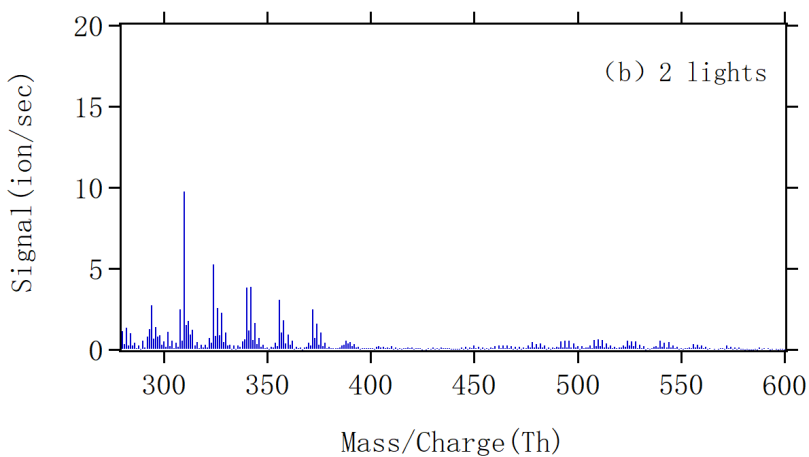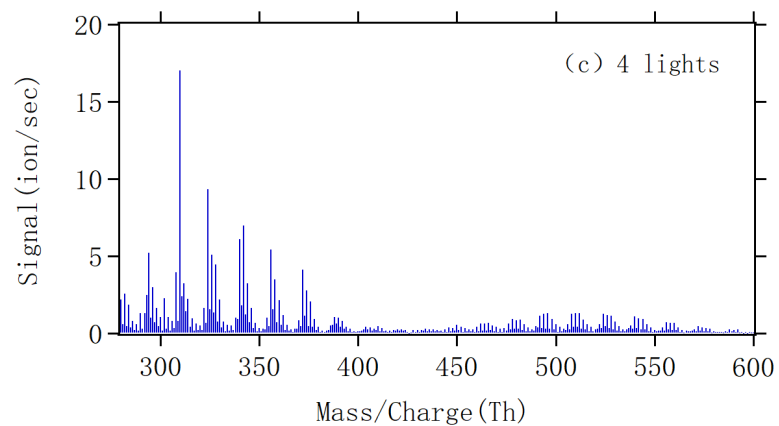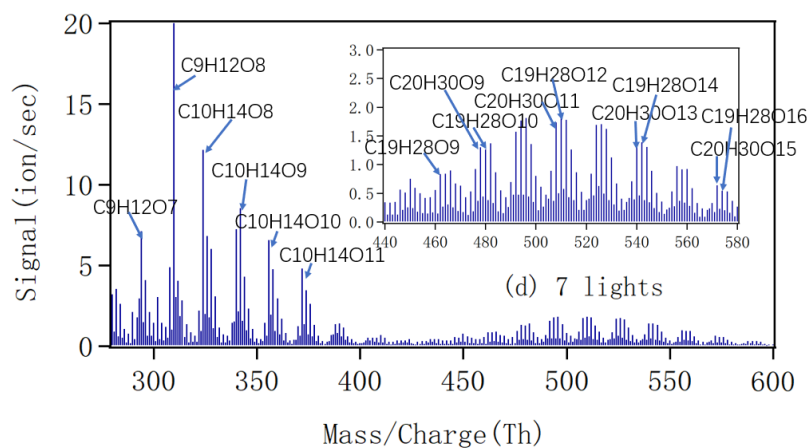
Figure 4. The mass spectra obtained by NO_3-CI-API-TOF during steady state with 1(a), 2(b), 4(c) and 7(d) lights. All peaks are detected as clusters with NO_3-. The spectra are plotted as unit mass resolution, with background signals removed, but the peak identifications (labeled in panel d) are based on high resolution analyses. The spectra correspond to the same four steady state conditions depicted in Fig. 2.

Atmospheric
Chemistry
and Physics
Discussions
Open Access
EGU
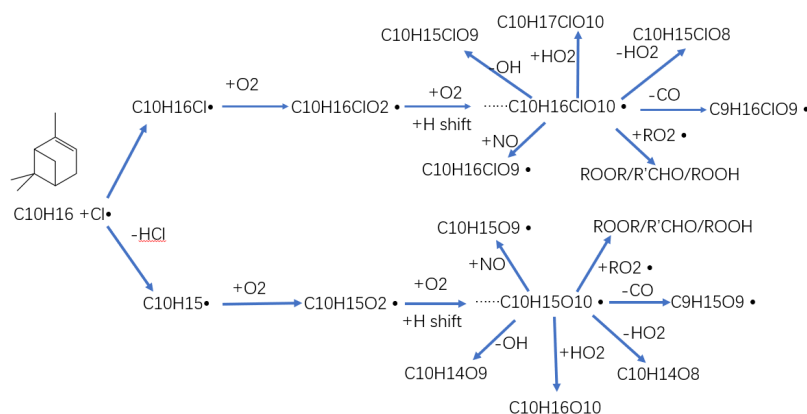
Figure 5. Proposed chemical pathways for chlorine radical oxidation of alpha-pinene, and subsequent autoxidation and HOM formation. The upper path shows the chlorine radical addition pathway, while the lower chain shows hydrogen atom abstraction pathway. In both cases, initially a C-centered radical forms ($C_{10}H_{16}Cl$ or $C_{10}H_{15}$) to which O_2 adds to form an initial peroxy radical. This peroxy radical may then undergo multi-step autoxidation to reach the example molecules $C_{10}H_{16}ClO_{10}$ or $C_{10}H_{15}O_{10}$ before termination. The observed HOM spectra in this study suggest a completely dominant role of the lower, H-abstraction, pathway for HOM formation.

644

645

646
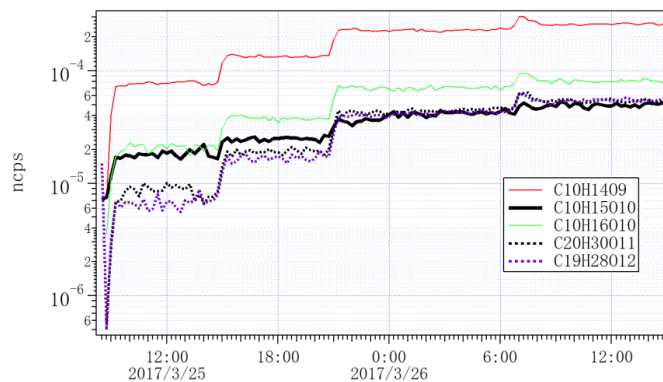
Figure 6. Time series of selected closed-shell HOM monomers, dimers and an RO_2 radical ($C_{10}H_{15}O_{10}$) detected by NO_3-CI-APi-TOF as the lights increased from 0 to 1, 2, 4 and 7.

650

651

652

653

654

655

656

657

658

659

660

661
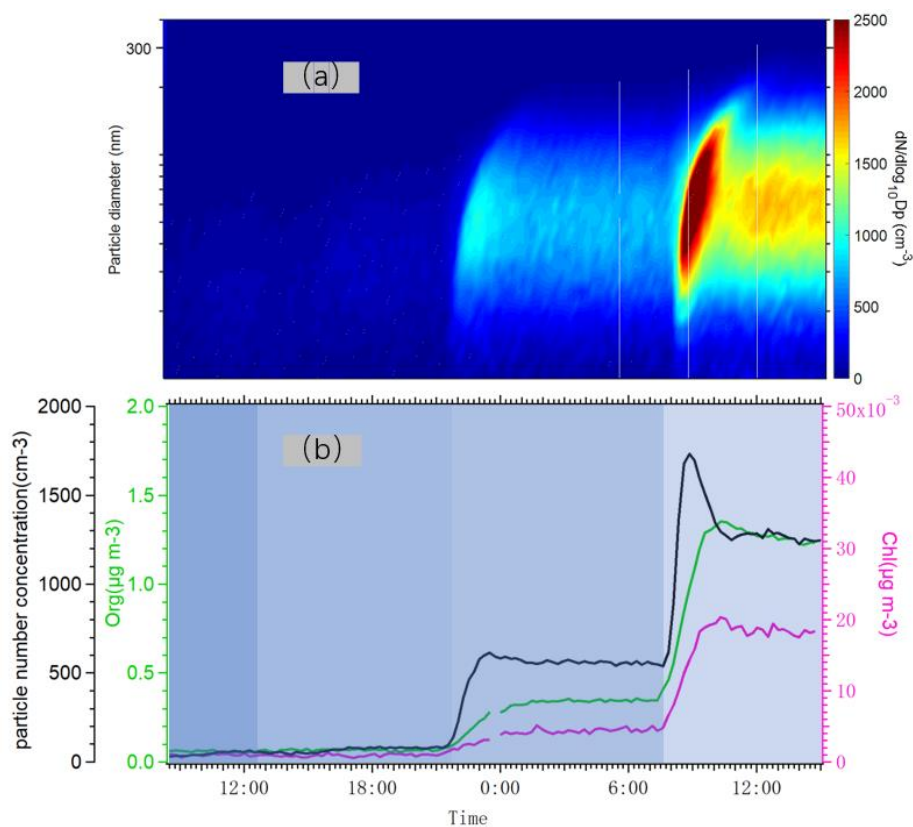
662

663

664   Figure 7. (a) Particle number size distribution measured by DMPS from 10 nm to

665   400nm when the lights varied from 1 to 2, 4 and 7. (b) Time series of total number

666   concentration (black) measured by DMPS, organic aerosol concentration (green) and

667   particulate chloride concentration (pink)measured by AMS.

668

669

670

671

672

673

674
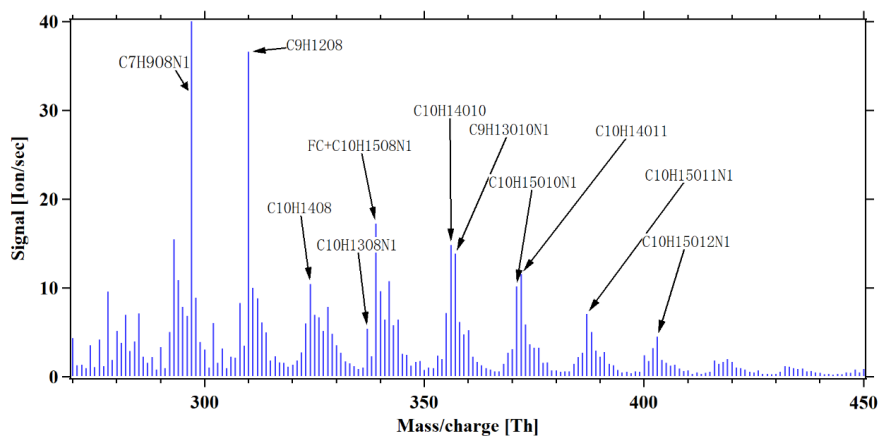
Figure 8. HOM mass spectrum during steady state alpha-pinene oxidation in the presence of 10 ppb NOx, with 7 lights switched on. In addition to molecules detected also in the experiments without NOx, several abundant organ nitrate peaks are formed. Note that a fluorinated compounds (FC) overlaps with the organ nitrate $C_{10}H_{15}O_8N$ at 339Th. All peaks are detected as clusters with NO_3^-.

680

681

682

683

684

685

686

687

688

689

690

691
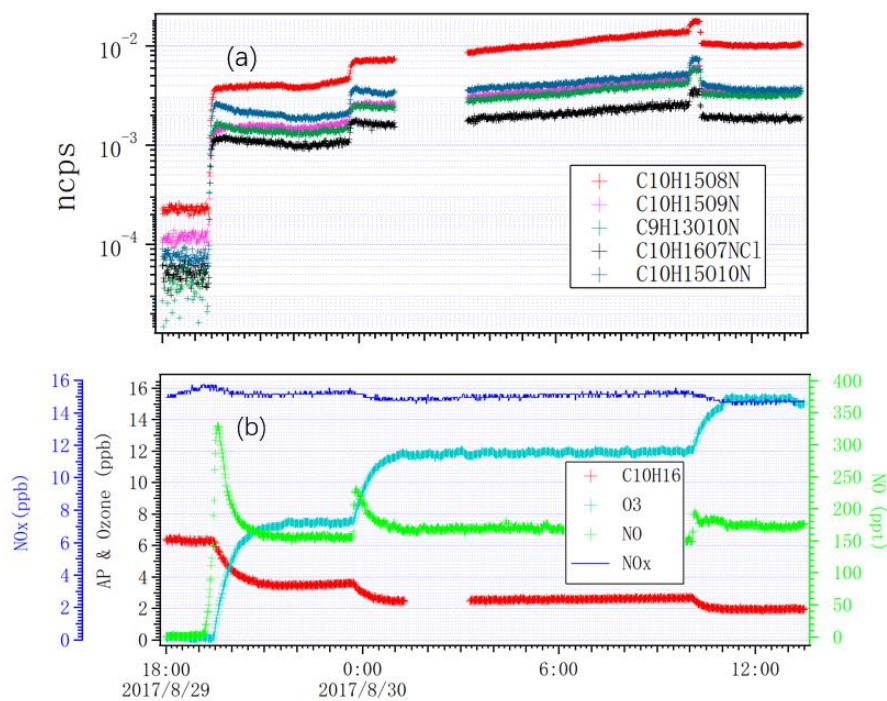
692

693

694   Figure 9. Time series of (a) selected HOMs measured by NO_3-CI-L-API-TOF and (b)
695   NO_x, a-pinene, ozone and NO, as the lights switched on from zero to 2, 4, and 7.

696

697

698

699

700

701

702

703
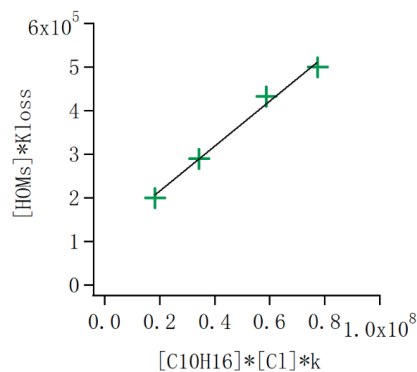
704

705

706   Figure 10. HOM loss rate ([HOM]*Kloss) as a function of the alpha-pinene

707   oxidation rate. In steady state the loss rate equals the formation rate, and thus

708   the slope of the points gives the molar yield of HOM from the alpha-pinene +

709   Cl reaction. The data corresponds to the conditions with 1, 2, 4 and 7 lights

710   switched on in the chamber, respectively. The slope indicates an average molar

711   yield of HOMs of 1.8%.

712

713

714